Improvement of aeroelastic stability of hingeless helicopter rotor blade by passive piezoelectric damping

Chul Yong Yun* and Seung Jo Kim**
School of Mechanical and Aerospace Engineering,
Seoul National University, Korea 151-742

Abstract

To augment weakly damped lag mode stability of a hingeless helicopter rotor blade in hover, piezoelectric shunt with a resistor and an inductor circuits for passive damping has been studied. A shunted piezoceramics bonded to a flexure of rotor blade converts mechanical strain energy to electrical charge energy which is dissipated through the resistor in the R-L series shunt circuit. Because the fundamental lag mode frequency of a soft-in-plane hingeless helicopter rotor blade is generally about 0.7/rev, the design frequency of the blade system with flexure sets to be so. Experimentally, the measured lag mode frequency is 0.7227/rev under the short circuit condition. Therefore the suppression mode of this passive damping vibration absorber is adjusted to 0.7227/rev. As a result of damping enhancement using passive control, the passive damper which consists of a piezoelectric material and shunt circuits has a stabilizing effect on inherently weakly damped lag mode of the rotor blades, at the optimum tuning and resistor condition.

Key Word : Piezoceramics, Shunt circuit, Passive damping, In hover, Hingeless helicopter, Lead-lag

Introduction

During the decade of the 1960's, by exploiting structural properties of advanced metallic and composite materials, the hingeless helicopter rotor systems replacing the flap and lead-lag hinges with flexures have been developed. By eliminating the flap and lag hinges, the hingeless rotor systems are mechanically simpler than the articulated rotor systems. The simplification reduces the weight and cost of the rotor system and increases its reliability and maintainability. But aeroelastic and areomechanical instabilities are still present and the auxiliary lead-lag damper in the rotor systems is needed to prevent their instabilities. Hingeless rotor systems can be divided into soft-in-plane rotor and stiff-in-plane rotor. For soft-in-plane blades, the fundamental lag bending mode frequency is less than the rotational frequency. For stiff-in-plane blades, lag frequency is greater than rotating speed. The advantage of the stiff-in-plane configuration is that it is not subjected to aeromechanical instabilities, such as ground and air resonance, and therefore it is not necessary to consider lag dampers in its design. However, stiff-in-plane rotor systems have the complex aeroelastic instabilities. Therefore the hingeless helicopter rotor systems are shifted toward soft-in-plane blades with lag damper, except very few helicopters, in spite of the its aeromechanical instabilities[1].

Much research has been made to make the soft-in-plane hingeless helicopter rotor stable from ground resonance and air resonance. Bousman[2,3] investigated aeroelastic and aeromechanical

* Research assistant, currently works for Korea Aerospace Research Institute
** Professor, Director of Flight Vehicle Research Center, corresponding author
E-mail : sjkim@snu.ac.kr Tel : 02-880-7388 Fax : 02-887-2662

stability of soft-in-plane hingeless rotor with kinematic coupling. He introduced pitch-lag coupling by using geometrically skewed flexure, and also introduced flap-lag coupling by changing pitch angle inboard of the flexures. And he showed that both flap-lag and pitch-lag coupling affect aeroelastic and aeromechanical stability of the hingeless helicopter rotor strongly. Han et al.[4] studied the ground resonance of the soft-in-plane hingeless helicopter rotor with composite flexures. They introduced the flap-lag coupling by changing flexure inclination angle and pitch-lag coupling by using bending-torsion coupling of the symmetric composite layers. And to represent the motion and structural stiffness of helicopter fuselage and landing gears, the gimbal was used. They showed that the combination of positive flap-lag coupling and negative pitch-lag coupling has a stabilizing effect on the ground resonance. Jung and Kim[5,6] investigated the effects of transverse shear and structural damping on the aeroelastic response of stiff-in-plane composite helicopter blade. They introduced the shear correction factor (SCF) to account for the sectional distribution of shear and improved the prediction of transverse shear behavior of composite. Those approaches are based on the aeroelastic coupling. Though the use of aeroelastic coupling is effective, the difficulties are the fact that aeroelastic couplings that may be effective for isolated blade stability may be ineffective in the presence of rotor body dynamic coupling. Another important factor is the number of different flight conditions and vehicle configurations that must be stable[7]. These difficulties come from the inherent weakly damped lag mode. If we can have the high structurally damped flexure, the instabilities of the blades may be less severe. And several researchers pursued the techniques to increase the structural damping. The methods are to incorporate high damping materials such as viscoelastic materials into the blade to increase the structural damping[7].

In this paper, to increase the structural damping of the flexures, the passive damping control using the piezoelectric materials is applied to rotor blades. In recent, piezoelectric passive control together with active control has been studied for the purpose of the vibration suppression. The characteristics of the piezoelectric are to transform mechanical vibration energy to electrical energy. In other words, the piezoelectric can be used as energy transformer. The transformed electrical energy can be dissipated into the heat energy by shunt circuits. Thus the vibrations could be suppressed. Hagood and von Flotow[8] have presented the passive control using the piezoelectric in detail. They introduced the simple shunting circuit consisting of a resistor and an inductance, which make an electrical resonance. As it is tuned optimally to vibration mode desired to damp, the structure vibration decreased effectively. In the paper, the analysis has been done by deriving the effective mechanical impedance for the piezoelectric element shunted by an arbitrary circuit. Hollkamp[9] expanded the theory so that a single piezoelectric element can be used to suppress multiple modes. Since that, several researchers[10,11] have studied the effects of the shunt circuit which is critical in passive damping using the piezoelectric devices.

The objective of this paper is to investigate stability characteristics of the hingeless rotor system by the increase of structural damping of the rotor blade using passive piezoelectric damping. First, the equations of motion of the piezoelectric with R-L elements in series shunt circuit will be derived on the basis of Hamilton's principle. The piezoelectric can be modeled as the voltage source in series to the inherent capacitance. And the governing equations of rotor blade will be presented and finite element method is used to solve the nonlinear equation. Finally, experiment of aeroelastic stability of rotor blade with the shunted piezoceramics in hover will be carried out.

Piezoelectric material

Equations of piezoelectric materials

The constitutive equations of piezoelectric materials in linear range for one-dimensional transverse loads are

$$\begin{Bmatrix} D \\ S \end{Bmatrix} = \begin{bmatrix} \varepsilon^T & d_{31} \\ d_{31} & s^E \end{bmatrix} \begin{Bmatrix} E \\ T \end{Bmatrix} \tag{1}$$

Here, the standard IEEE notation is used. The equation (1) represents electrical charge quantity per unit area and strain on the piezoelectric materials when electrical fields and stresses are applied. And at equation (1), the first row is applied when the piezoelectric materials are used as sensors and the second is applied when they are used as actuators. Therefore equation (1) is usually used for the active control with the piezoelectric. For the passive control with them, mechanical displacement or strain S and electrical displacement or electrical charge density D are considered as the independent variables. Therefore when strain and electrical charge density are applied, electrical field and stress on the materials can be expressed as follows

$$\begin{Bmatrix} E \\ T \end{Bmatrix} = \begin{bmatrix} \frac{1}{\varepsilon^S} & -h_{31} \\ -h_{31} & c^D \end{bmatrix} \begin{Bmatrix} D \\ S \end{Bmatrix} \tag{2}$$

Where h_{31} known as piezoelectric stress coefficient means that it is the electrical field appearing across the piezoelectric when unit strain is applied at constant charge. And c^D is young's modulus when the materials are in the open shunted condition. The piezoelectric stress constant h_{31} can be expressed in terms of electromechanical coupling coefficient k_{31} as follows:

$$h_{31} = \sqrt{\frac{c^D}{\varepsilon^S}} k_{31} \tag{3}$$

The electromechanical coupling coefficient k_{31} is expressed as $k_{31} = d_{31} / \sqrt{s^E \varepsilon^T}$. In the single-degree-of-freedom setting, the constitutive equations of the piezoelectric material can be rewritten:

$$\begin{Bmatrix} V \\ F \end{Bmatrix} = \begin{bmatrix} \frac{1}{C_P^S} & -H \\ -H & K_P^D \end{bmatrix} \begin{Bmatrix} Q \\ X \end{Bmatrix} \tag{4}$$

Q and X are charge and displacement of the piezoelectric, respectively. And V and F are voltage appearing across the material and internal elastic force of the material, respectively. $C^S{}_P$ is the capacitance of the material under constant strain, and $K^D{}_P$ is the stiffness in the open circuit condition and H is the electro-mechanical coupling. The electro-mechanical coupling H can be expressed in terms of stiffness, capacitance and electromechanical coupling coefficient k_{31} of the piezoelectric.

$$H = \sqrt{\frac{K_P^D}{C_P^S}} k_{31} \tag{5}$$

The equation of the motion of the piezoelectric connected to shunt circuit consisting of R-L elements in series can be derived from the Hamilton's principle. That is

$$\int_{t_1}^{t_2} [\delta(T - V + W)] dt = 0 \tag{6}$$

For shunt circuit, the kinetic energy T and the potential energy V include not only the effect of the mechanical displacement and velocity, but also the magnetic and electromagnetic effect. So the kinetic energy and the potential energy are

$$T = \frac{1}{2} M \dot{X}^2 + \frac{1}{2} L \dot{Q}^2 \tag{7a}$$

$$V = \frac{1}{2} FX + \frac{1}{2} VQ = \frac{1}{2} K_P^D X^2 + \frac{1}{2} \frac{1}{C_P^S} Q^2 - HQX \tag{7b}$$

Where total kinetic energy T consists of the mechanical kinetic energy and the electrical kinetic energy, and total potential energy V consists of the mechanical potential energy, the electrical potential energy, and the potential energy coupled electric fields and mechanical fields.

The virtual work consists of the heat dissipation through the resistor and externally applied force.

$$\delta W = -R\dot{Q}\delta Q + f\delta X \tag{8}$$

If the equation (7a), (7b) and (8) are substituted into the equation (6) and integration by part are carried out, the equation of motion of the shunted piezoelectric can be expressed as follows:

$$M\ddot{X} + K_P^D X - HQ = f \tag{9a}$$

$$L\ddot{Q} + R\dot{Q} + C_P^{S^{-1}} Q - HX = 0 \tag{9b}$$

The equation (9a) represents the mechanical behavior of the piezoelectric materials whose actuating force is HQ. The mechanical vibration of the piezoelectric causes the electrical charges on the both electrodes of the material and this charge induces the actuating force that reacts to the structure to suppress the vibration. The equation (9b) shows that it is the electric circuit which consists of L-R-C elements in series with the voltage source as HX. Because of mechanical deformation the voltage difference appears across the electrodes of the piezoelectric and it plays a role in the voltage source. Therefore shunted piezoelectric device can be considered as the electric circuit, as shown in the figure 1, which consists of the voltage source, the capacitance that are inherent characteristics of piezoelectric material, the resistance, and the inductance that are shunted. From the Kirchhoff's Voltage Law, the voltage of the source HX drops through the capacitor, the resistor and the inductor, respectively. In the equation (9b), the first term is the voltage in the inductance, the second is the voltage in the resistor and the third is the voltage in the inherent capacitor. In the electric circuit, the inductor makes the circuit have electrical resonance with the capacitor of piezoelectric materials itself and the resistor takes a role in heat dissipation. In other words, the mechanical vibration energy is transformed into the electric energy by the piezoelectric material and this is dissipated through resistor into heat energy. Therefore the vibration can be damped out.

In the short circuit without a resistor and an inductor, the electrical equation (9b) becomes

$$C_P^{S^{-1}} Q - HX = 0 \tag{10}$$

If this equation is used, the mechanical equation (9.a) can be expressed in terms of the mechanical displacement X and then the stiffness of the shunted piezoelectric becomes

$$K_P^E = (1 - k_{31}^2) K_P^D \tag{11}$$

This is the stiffness of the short circuit piezoelectric. An open circuit piezoelectric is stiffer than a short circuit since it stores energy as electrical energy and returns it back to the structure as mechanical energy.

The modeling of structures bonded to piezoelectric materials

The structures bonded to patch-like piezoelectric materials can be considered as the mass-spring model by simply considering modal quantities of single degree of freedom in the case that modes are well separated. The whole systems which are structures with piezoelectric materials are that the modal stiffness of the piezoelectric material is parallel to that of the structure and the modal mass of the rotor blade plus that of the piezoelectric materials is total modal mass as shown in figure 3. Then the equations of the systems can be written like below:

$$M\ddot{X} + (K_S + K_P^D) X - HQ = f \tag{12a}$$

$$L\ddot{Q} + R\dot{Q} + C_P^{S^{-1}} - HX = 0 \tag{12b}$$

Where K_S and $M$are the modal stiffness of host structures and the total modal mass, respectively. This is the governing equation of structures bonded to piezoelectric materials with R-L in series shunt circuit. In the equation (12.a), the modal stiffness is expressed in terms of the stiffness of open shunted piezoelectric materials. However, the equation can be rewritten in terms of the stiffness of short shunted piezoelectric materials. Using the relation (11), the relation of the total modal stiffness between open circuit system and short circuit system is

$$\frac{K_S + K_P^D}{K_S + K_P^E} = 1 + \frac{K_P^E}{K_S + K_P^E}\frac{k_{31}^2}{1 - k_{31}^2} \tag{13}$$

From the second term in right hand side, the generalized electromechanical coupling coefficient K_{31}, is defined as

$$K_{31}^2 = \frac{K_P^E}{K_S + K_P^E}\frac{k_{31}^2}{1 - k_{31}^2} \tag{14}$$

It is the fraction of the system modal strain energy which is converted into electrical energy by the open circuit piezoelectric.

Optimum resistance and inductance

To find characteristics of the system that are natural frequency and damping, natural vibration analysis is needed. Assuming the displacement and the charge harmonic motion e^{st}, the characteristic equation of the governing differential equations (12) is as follows:

$$\Delta(s) = \left\{Ms^2 + (K_S + K_P^D)\right\}\left\{Ls^2 + Rs + \frac{1}{C_P^S}\right\} - H^2 = 0 \tag{15}$$

For simplification, non-dimensional parameters are introduced like below

$$\omega_e = \frac{1}{\sqrt{LC_P^S}},\ \omega_n^E = \sqrt{\frac{K_S + K_P^E}{M}},\ \delta = \frac{\omega_e}{\omega_n^E},\ r = RC_P^S\omega_n^E,\ \lambda = \frac{s}{\omega_n^E} \tag{16}$$

Where ω_n^E is the natural frequency of a short circuit piezoelectric system, ω_e is electric resonant frequency, is the tuning parameter and r is damping parameter. Using the non-dimensional parameters and the relation (11), the equation (15) can be rewritten as follows:

$$\begin{aligned}&(\lambda^2 + 1 + K_{31}^2)(\lambda^2 + r\delta^2\lambda + \delta^2) - \delta^2 K_{31}^2 \\ &= \lambda^4 + r\delta^2\lambda^3 + (1 + K_{31}^2 + \delta^2)\lambda^2 + (1 + K_{31}^2)r\delta^2\lambda + \delta^2 = 0\end{aligned} \tag{17}$$

The natural frequency and damping should be determined by solving the fourth-order polynomial equation (17).

Now, optimum resistance and inductance must be determined in order to suppress the vibration effectively. In a shunt circuit, inductance increases current in alternating voltage source by making resonant frequency tuned to the natural frequency of the system and a resistance dissipates the electric energy.

In this paper, pole placement method[8] to determine optimum resistance and tuning inductance is used. In the equation (17), at a given K_{31}, as the damping parameter is increased the distinct poles can coalesce only if a special value of the tuning parameter is chosen. This point of coalescence is the optimized r and δ. Since the poles are double conjugate pairs, letting the two poles of coalescence λ_1, λ_2, the characteristic equation can be expressed below:

$$(\lambda - \lambda_1)^2(\lambda - \lambda_2)^2 = 0 \tag{18}$$

Comparing the equation (17) with the equation (18) term by term, optimum tuning parameter and optimum damping parameter are as follows:

$$\delta_{opt} = 1 + K_{31}^2 \tag{19}$$

$$r_{opt} = 2\sqrt{\frac{K_{31}^2}{(1 + K_{31}^2)^3}} \tag{20}$$

Using the definitions of the tuning parameter and the damping parameter, the optimal inductance and the optimal resistance are

$$L_{opt} = \frac{1}{C_P^S(\omega_n^E \cdot \delta_{opt})^2} \tag{21}$$

$$R_{opt} = \frac{r_{opt}}{C_P^S \omega_n^E} \tag{22}$$

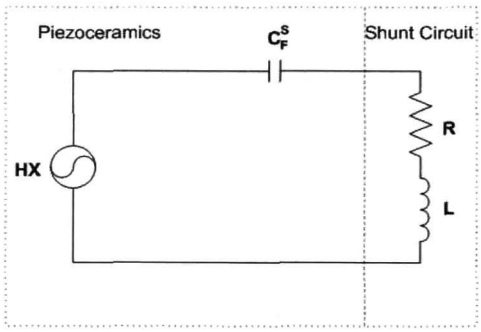

Fig. 1. Shunted piezoelectric electrical model

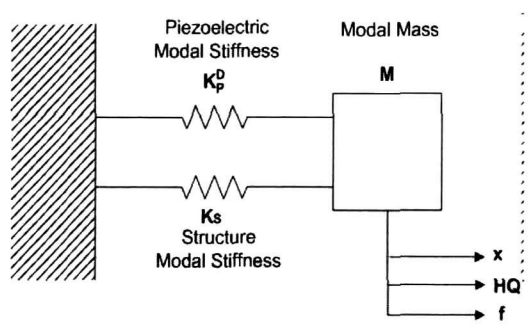

Fig. 2. Single degree of freedom model of system

Rotor blade

Though the motion of piezoelectric system is known, the equations of the rotor blade must be derived to know the characteristics of rotor blades with the piezoelectric device. Helicopter rotor blade can be considered as one dimensional straight cantilever beam rotating at constant speed since it is very long in a spanwise direction comparing to in a chordwise direction. And in deriving a nonlinear system of equations, ordering scheme is applied to avoid overcomplicating the equation of motion.

Governing equations of rotor blade

The equations of motion of rotor blade are developed by Hamilton's principle. Hamilton's principle may be expressed as

$$\delta\Pi = \int_{t_1}^{t_2} [\delta U - \delta T - \delta W]dt = 0 \tag{23}$$

Where U is the strain energy, T is the kinetic energy, and W is the virtual work of the external forces. The first variation of the strain energy and the first kinetic energy are derived in Hodges and Dowell's report[12]. The virtual work W of the nonconservative forces may be expressed as

$$\delta W = \int_0^R (L_u \delta u + L_v \delta v + L_w \delta w + M_\phi \delta\phi)dx \tag{24}$$

Where L_u, L_v, L_w, and M are the distributed loads that act in the span, lead-lag, and flap directions and the aerodynamic pitching moment about the undeformed elastic axis, respectively. Two-dimensional quasi-steady aerodynamic theory is used to evaluate aerodynamic forces. Non-circulatory-origin aerodynamic components due to apparent mass effect are also considered.

The equations of the blade based on the Hamilton's principle can be solved by the finite element method. The blade is discretized into a number of beam elements. Each beam element consists of fifteen degrees of freedom. These degrees of freedom are distributed over element nodes (2 boundary nodes and 3 interior nodes). There are six degrees of freedom at each element boundary node. These six degrees of freedom correspond to u , v , v′ , w , w′ , and $\hat{\phi}$. There are two internal nodes for axial deflection u , and one internal node for elastic twist $\hat{\phi}$ [Fig. 3]. Between elements there is continuity of displacement and slope for flap and lag bending deflection, and continuity of displacement for elastic twist and axial deflections. This element insures physically consistent linear variations of bending moments and torsional moment, and quadratic variation of axial force within each element. Those are summarized about k-th element as follows:

$$u = \sum_{i=1}^{4} H_i^u u_i \quad , \quad v = \sum_{i=1}^{4} H_i v_i \quad , \quad w = \sum_{i=1}^{4} H_i w_i \quad , \quad \hat{\phi} = \sum_{i=1}^{3} H_i^{\phi} \hat{\phi}_i \tag{25}$$

Where subscript i denotes i-th node of k-th element and H_i^u, H_i are the third order polynomial functions and H_i^{ϕ} is the quadratic polynomial function.

Because the virtual displacement in the virtual energy expression is independent of time, the virtual energy expression in equation (24) is written in the discretized form such that

$$\sum_{k=1}^{N_e} (\delta U_k - \delta T_k - \delta W_k) = 0 \tag{26}$$

Where N_e is total number of beam elements. Substituting equation (25) into the discretized Hamilton's principle form equation (26), and generalized coordinate $\mathbf{q}_i$ taken below

$$\mathbf{q}_i^T = [u_1\ u_2\ u_3\ u_4\ v_1\ v_1'\ v_2\ v_2'\ w_1\ w_1'\ w_2\ w_2'\ \hat{\phi}_1\ \hat{\phi}_2\ \hat{\phi}_3]$$

Finally, the equations of blade are as follows:

$$\mathbf{M(q)}\ \ddot{\mathbf{q}} + \mathbf{C(q)}\ \dot{\mathbf{q}} + \mathbf{K(q)q} = \mathbf{F} \tag{27}$$

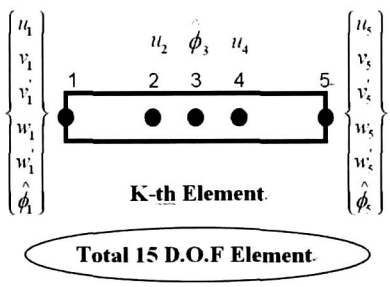

Fig. 3. Finite element model

Method solving the governing equation

The perturbation method which assumes a small disturbance from the equilibrium operating conditions may be used to analyze blade stability from the finite element equation (27). Generalized coordinate **q** can be expressed in terms of steady equilibrium quantity $\mathbf{q}_0$ and small unsteady perturbation quantity **q**. Substituting the generalized coordinate into equation (27) and ignoring the terms with time, the static equilibrium equation can be found such that

$$\mathbf{K}(\mathbf{q}_0)\mathbf{q}_0 = \mathbf{F} \tag{28}$$

This nonlinear equilibrium equation which includes the variable desired to solve in the stiffness matrix is solved by the Newton-Raphson method. The static solution defines the equilibrium deflections. The second equation is obtained by substituting the generalized coordinate into the modal equation

(27), subtracting the equilibrium equation, and discarding all nonlinear products of perturbation quantities. The coefficients of these linearized perturbation equations are functions of the equilibrium solution. The perturbation equations define the unsteady blade motion near the equilibrium operating condition. The perturbation equations are linear, homogeneous, constant-coefficient ordinary differential equations of the form

$$\mathbf{M}(\mathbf{q}_0)\delta\ddot{\mathbf{q}} + \mathbf{C}(\mathbf{q}_0)\delta\dot{\mathbf{q}} + \mathbf{K}(\mathbf{q}_0)\delta\mathbf{q} = \mathbf{0} \tag{29}$$

From this equation, the aeroelastic instabilities can be determined. Since we are primarily concerned with lower frequency instabilities, modal reduction transformation may be found by considering free vibration of the blade about the equilibrium operating condition. With the modal matrix of eigenvectors for the free vibration of the motion, transformation of the generalized coordinate $\mathbf{q}$ into the modal coordinate $\mathbf{x}$ is $\mathbf{q}=\mathbf{x}$ and the equation (29) is transformed and thus modal flutter equation can be obtained such that

$$\overline{\mathbf{M}}\ddot{\mathbf{x}} + \overline{\mathbf{C}}\dot{\mathbf{x}} + \overline{\mathbf{K}}\mathbf{x} = \mathbf{0} \tag{30}$$

Changing the equation (30) into state form of the first order differential equation, it is

$$\begin{Bmatrix}\dot{\mathbf{x}}\\ \ddot{\mathbf{x}}\end{Bmatrix} = \begin{bmatrix}\mathbf{0} & \mathbf{I}\\ -\overline{\mathbf{M}}^{-1}\overline{\mathbf{K}} & -\overline{\mathbf{M}}^{-1}\overline{\mathbf{C}}\end{bmatrix}\begin{Bmatrix}\mathbf{x}\\ \dot{\mathbf{x}}\end{Bmatrix} = \mathbf{P}\begin{Bmatrix}\mathbf{x}\\ \dot{\mathbf{x}}\end{Bmatrix} \tag{31}$$

The characteristics of rotor blade can be determined by carrying out the eigenvalue analysis of the modal matrix $\mathbf{P}$.

Experiment of rotor blade

Blade

The experimental system, ERASA(Experimental Rotor Aeroelastic Stability Apparatus) shown in figure 5 is composed of the 4-bladed small scale hingeless rotor of 2 meter diameter. The properties of the blades are that the cross section type is NACA 0012, chord/radius is 0.0722, lock number is 2.436, solidity ratio is 0.0615, and nominal rotating speed is 600 RPM. Individual hingeless rotor consists of the blade which is made of composite material and the flexure which is between the blade and the hub. The fundamental lag mode frequency of a soft-in-plane hingeless helicopter rotor blade is generally about 0.7/rev. Thus the flexures are designed such that rotating lag frequency at 600 RPM is about 7 Hz. To investigate improvement of stability of the rotor blades using the piezoelectric with shunt circuit experimentally, the piezoceramics are bonded to surfaces of the flexures as shown in figure 4. The flexures of which dimensions are 14 mm width, 120 mm length, and 4 mm thickness are made of the aluminum alloy 7075 and the piezoceramics plates with the dimensions of 14 mm width, 50 mm length, and 0.5 mm thickness are manufactured by FUJI CERAMICS Co.. The material properties of the flexure and piezoceramics are presented in Table 1. Two pieces of the piezoceramics are bonded to each surface of the flexure and thus 4 pieces of the piezoceramics

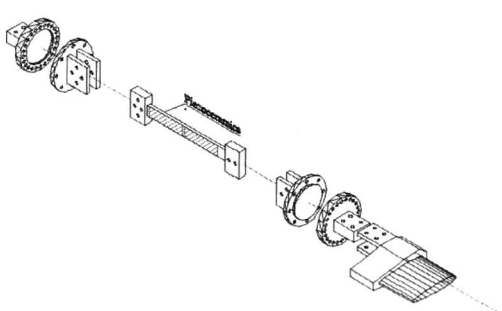

Fig. 4. Piezoceramics bounded to flexure

Table 1. The material properties of flexures and piezoceramics

Flexure	Young's modulus Density	E=72.3 G ρ=2906 kg/m^3
Piezoceramics	Young's modulus (short) Dielectric constant Coupling coefficient Transverse d constant Capacitance Density	E=59 G ε^T=3400 ε^0 k_{31}=0.36 d_{31}=260e-12 m/V C_P^S = 42.6 nF ρ=7400 kg/m^3

are bonded to each flexure. Total 16 pieces of the piezoceramics are used in all rotor blades. One side of the each piezoceramics is grounded to the flexure and the other side is connected to shunt circuit. The ground of shunt circuit is connected to the flexure. Shunt circuit consists of R-L in series. For experiment, very large value of inductance L is needed. It would not be practical to realize by classical means. However, a tunable active inductor that is synthetic can be realized electronically to use op-amp, capacitors, and resistors[13].

Data acquisition and procedure

In experiment on aeroelastic stability of hingeless rotor blade in hover, it is important to excite the lag mode since this mode instabilities are critical. Excitation is applied with cyclic pitch system and the exciting frequency is regressing lag mode. After sufficient amplitude of blade motion is achieved, at which point the excitation is cut off and the motion is allowed to decay. Strain gages are used to sense the blade lag motion. The strain gages attached on the piezoceramics form quarterbridges to sense the lag mode which is inherent weakly damped. The signals from the strain gages are transmitted to the 36-pole slip-ring, and then those signals are passed to strain conditioning amplifier where amplified 1000 times and filtered. And it is necessary to filter those signals for eliminating high frequency noise from AC servo motors(main motor and the motor for changing collective pitch of the blade) and step motor(for exciting cyclic pitch of the blade). The moving block method[14,15] is used to compute frequency and damping from the strain gages signals. The only one critical mode is considered in most test situations. In this method, the response amplitude corresponding to the desired frequency is analyzed on block sizes of the digital data using a Fast Fouries Transform. Each response amplitudes are calculated by moving the data block (generally half sizes of sample datum) by one sample at a time. From the natural log plot of response amplitude with time, the damping is estimated using a linear least square fit to the resultant curve. Using this damping estimating technique, in experiments, 1,024 signals are sampled at 100 Hz sampling rate by using 16 channel data acquisition system. Moving block analysis is done with the Labview VIs (Virtual Instruments). The procedure for the experiment in hover is shown in Figure 6. And at least ten transient records were obtained.

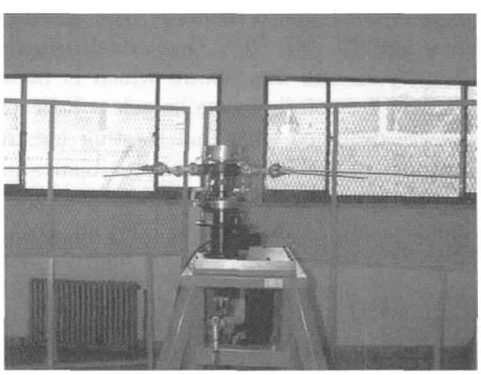

Fig. 5. Experimental Rotor Aeroelastic Stability Apparatus (ERASA)

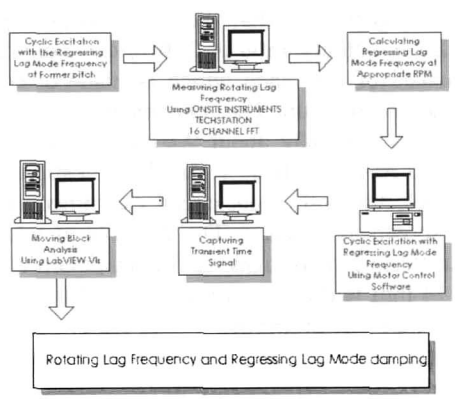

Fig. 6. Experimental procedure

Results of experiment

Experiment to improve aeroelastic stability of the rotor blades in hover using the piezoelectric with shunt circuit has been carried out. The frequencies of rotating rotor blades increase because of stiffening effect due to centrifugal forces. Thus helicopter has many possibilities of the instabilities from the resonance, such as ground resonance, air resonance, and resonance with rotating speed and so on. Design of helicopter rotor blades must be avoided from such instabilities. Figure 7 shows fanplot which plots the fundamental mode frequencies with rotating speed. The nonrotating lag frequency is 3.750 Hz under short circuit condition and as rotating speed increases, the lag mode frequency

is also increased by centrifugal force and thus the frequency reaches 7.227 Hz at the operating speed 600 RPM. About 300 RPM the fundamental lag mode coalesces into the rotating speed, at which lag mode was excited by itself without cyclic excitation.

In passive control with shunted piezoelectric, it is important to find the generalized electromechanical coupling coefficient K_{31}. Experimentally, it can be found from the following equation

$$K_{31}^2 = \left(\frac{\omega_n^D}{\omega_n^E} \right)^2 - 1 \tag{32}$$

At 600 RPM, when shunt circuit is open and short, the lag mode frequency is 7.324 Hz and 7.227 Hz, respectively. Using the equation (32), K_{31} is 0.164. From the frequencies at open and short circuits and the capacitance, optimum inductance L_{opt} is 5,400 H and optimum resistance R_{opt} is 82 kΩ. Figure 8 shows time domain signals during about 10 seconds of the blade with open shunted piezoceramics. From the time history, we obtain the value of damping coefficient, 0.3 %, using moving block analysis. Figure 9 is the time history of the blades with optimum shunted piezoceramics. At this case, damping coefficient is about 0.65 %. There is more than 2 times damping enhancement in optimum shunting.

Figure 10 shows that the lag mode damping increases as the collective pitch increases. If the pitch increases, then aerodynamic drag is increased and thus damping increases. And structural damping due to passive shunted piezoelectric shifts upward the plot of lag mode damping with collective pitch.

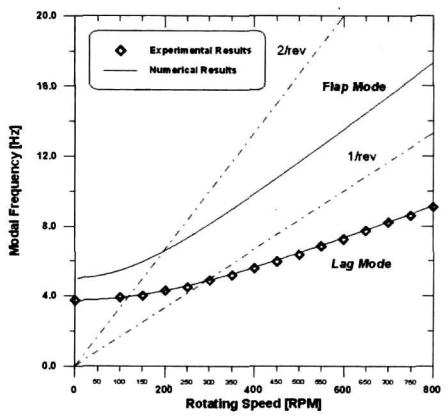

Fig. 7. Fanplot of lag mode frequency with rotating speed

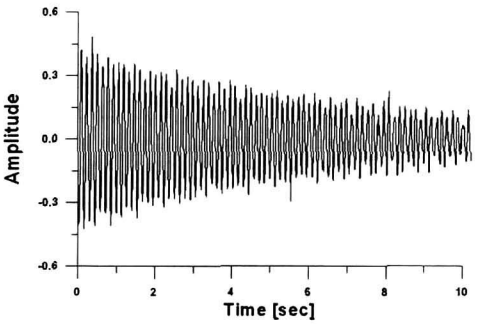

Fig. 8. Time history at open circuit

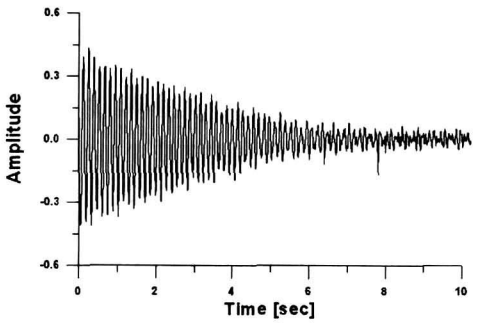

Fig. 9. Time history with optimum shunt circuit

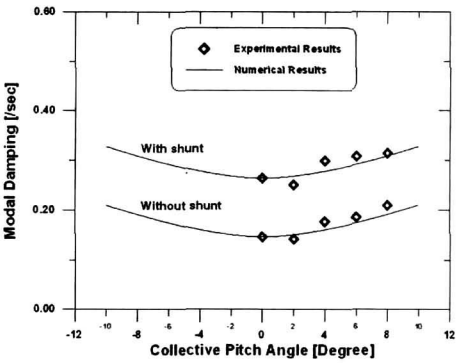

Fig. 10. Plot of the lag mode damping with collective pitch angle in the cases of the shunt and no shunt

Conclusions

To augment weakly damped lag mode stability of soft-in-plane hingeless helicopter rotor blade, piezoelectric shunt with a resistor and an inductor for passive damping has been studied. The equations of the motion of the shunted piezoelectric are derived on the basis of Hamilton's principle. From this equations, the shunted piezoelectric which actuates the structures in proportional to generating charge leads the vibration to be suppressed. And the mechanical vibration makes the piezoelectric be alternating voltage source in the circuit which consists of the piezoelectric and R-L series connection. The frequency of the voltage source which is equal to the frequency of a vibration mode becomes close to electrical resonance and then current in the circuit increases so that electrical energy is more dissipated.

Helicopter rotor blades experience many different flight conditions so that it must be stable from all the conditions. The use of the shunted piezoelectric to increase the structural damping will make the blades stable in most flight conditions simply tuning the shunt circuit to the conditions. To investigate the efficiency, experiment to improve aeroelastic stability of the rotor blades in hover using the piezoelectric with shunt circuit was carried out. The results of experiment are that there is 217% increment of damping value. The passive damping using the shunted piezoelectric is sensitive to the value of the inductance. Especially, for lower mode suppression of vibration, it must be careful to tune the electrical resonance to the mode. Then higher damping could be achieved through better optimized tuning of shunt circuit.

References

1. Ormiston, R. A., "Investigations of Hingeless Rotor Stability", *Vertica*, Vol. 7, No. 2, 1983, pp. 143~181.

2. Bousman, W. G., Sharpe, D. L. and Ormiston, R. A., "An Experimental Study of Techniques for Increasing the Lead-Lag Damping of Soft In-plane Hingeless Rotors", Preprint No. 1035, Preceedings AHS 32nd National Forum, Washington D.C., May 1976.

3. Bousman, W. G., "The Effects of Structural Flap-Lag and Pitch-Lag Coupling on Soft In-plane Hingeless Rotor Stability in Hover," NASA TP 3002, AVSCOM TR 89-A-002, 1990.

4. Han, C. H., Yoon, C. Y., Moon, S. W., Lee, C. S., Jung, S. N., Lee, H. K. and Kim, S. J., "Experimental and Numerical Investigation on Helicopter Ground Resonance with Composite Flexures", 24th European Rotorcraft Forum, Vol. 2 DY04, September 1998.

5. Jung, S. N. and Kim, S. J., "Aeroelastic Response of Composite Rotor Blades Considering Transverse Shear and Structural Damping", AIAA Journal, Vol. 32, No, 4, 1994, pp. 820~827.

6. Jung, S. N. and Kim, S. J., "Effect of Transverse Shear on Aeroelastic Stability of a Composite Rotor Blade", AIAA Journal, Vol. 33, No. 8, 1995, pp. 1541~1543.

7. Ormiston, R. A., "The Challenge of the Damperless Rotor", Proceedings of the 22nd European Rotorcraft Forum, Brighton, England, September 17-19, 1996.

8. Hagood, N. W. and Flotow, F. F., "Damping of Structural Vibrations with Piezoelectric Materials and Passive Electrical Networks", Journal of Sound and Vibration, Vol. 146, No. 2, 1991, pp. 243~268.

9. Hollkamp, J. J., "Multimode Passive Vibration Suppression with Piezoelectric Materials and Resonant Shunts", Journal of intelligent Material Systems and Structures, Vol. 5, 1994, pp. 49~57.

10. Agnes, G. S. and Inman, D. J., "Nonlinear Piezoelectric vibration Absorbers", Proceeding's of SPIE, Vol. 2720, 1996, pp. 247~258.

11. Wu, S., "Piezoelectric shunts with a parallel R-L circuit for structural damping and vibration control", Proceedings of SPIE, Vol. 2720, 1996, pp. 259~269.

12. Hodges, D. H. and Dowell, E. H., "Nonlinear Equations of Motion for the Elastic Bending and Torsion of Twisted Nonuniform Rotor Blades", NASA TN D-7818, Dec. 1974.

13. Chen, W. K., Passive and Active Filters, John Wiley, New York, 1994.

14. Bousman, W. G. and Winkler, D. J., "Application Of The Moving-Block Analysis", AIAA Dynamics Specialists Conference, April 9-10, 1981.

15. Tasker, F. A. and Chopra, I., "Assessment of Transient Analysis Techniques for Rotor Stability Testing", Journal of the American Helicopter Society, Vol. 35, No. 1, 1990, pp. 39~50.